Alternative co-initiators for photocurable dental resins

Hamidi, Ali; Hadis, Mohammed; Palin, Will

DOI:
10.1016/j.dental.2022.06.001

Document Version
Peer reviewed version

Citation for published version (Harvard):
Hamidi, A, Hadis, M & Palin, W 2022, 'Alternative co-initiators for photocurable dental resins: polymerisation, quantum yield of conversion and cytotoxicity', *Dental Materials*, vol. 38, no. 8, pp. 1330-1343. https://doi.org/10.1016/j.dental.2022.06.001

Alternative co-initiators for photocurable dental resins: polymerisation, quantum yield of conversion and cytotoxicity.

Hamidi AS, Hadis MA, Palin WM
Dental and Biomaterials Science, College of Medical and Dental Science, Institute of Clinical Sciences, University of Birmingham, 5 Mill Pool Way, Edgbaston, Birmingham B5 7EG, UK

Abstract

Objectives: Cyclic acetals such as are naturally occurring compounds capable of acting as co-initiators during free-radical polymerisation, and potentially serve to offer non-allergic and biologically less toxic alternatives to conventional (tertiary) amines. The current study aimed to evaluate the polymerization efficiency and potential toxicity of cyclic acetals compared with conventional photoinitiator systems in photocurable dental resins. Methods: Both, 1,3 benzodioxole (BZD) and piperonyl alcohol (PA) were used in 0.5, 1.0, 1.5, 2.0, 3.0, 4.0 and 6.0 mol % concentrations. Whereas, N-phenyl glycine (NPG) was utilised in 0.5, 1.0, 1.5, 2.0, 3.0, 4.0 mol % concentrations for photopolymerisation of an unfilled model resin system, BisGMA and TEGDMA (1:1 mass %), involving three separate camphorquinone (CQ) concentrations of 0.5 (Low), 1.0 (Intermediate) and 1.5 (High) mol %. Conventional tertiary amines; ethyl-4-dimethyamino benzoate (EDMAB) and dimethylaminoethyl methacrylate (DMAEMA) were utilised for comparison. Real-time degree of conversion (DC, %) was evaluated using Fourier transform near-infrared spectroscopy and quantum yield of conversion of CQ was calculated using UV-Vis spectroscopy. Cytotoxicity of NPG and cyclic acetals were assessed using MTT to determine metabolic activity of human dental pulp cells (HDPCs). Results: The cyclic acetals were capable of facilitating free radical polymerisation as co-initiators at all three CQ concentrations. Furthermore, the use of NPG as a co-initiator resulted in post-irradiation DC (%) that were comparable to both EDMAB and DMAEMA for all CQ concentrations. Alternative compounds facilitated the hydrogen abstraction process, which provided high conversion of CQ molecules. Quantum yield increased from 0.009 ± 0.0001 (0.5 mol %) to 0.03 ± 0.006 (6.0 mol %), and 0.01 ± 0.0003 (0.5 mol %) to 0.04 ± 0.001 (6.0 mol %), for respective BZD and PA formulations involving 1.0 mol % CQ. The use of NPG led to relatively higher quantum yield values (Up to 0.09 ± 0.007 at 4.0 mol %) , though it exhibited competitive effects in absorbing blue light, which might be attributed to the photolytic degradation of NPG and the formation of N-methylaniline. MTT assay indicated alternative co-initiators to be comparatively less cytotoxic than EDMAB and CQ. Relative metablic activity of HDPCs treated with BZD, PA, and NPG eluates were 58.3 ± 15.7, 57.5 ± 17.4 and 64.6 ± 12.2 %, when compared with untreated HDPCs group (Control), respectively. Exposure to DMAEMA-based eluate led to relative metabolic activity (60.0 ± 0.5 %) that was comparable to that of cyclic acetals. Treatment with neat model resin eluate displayed the highest relative reduction in metabolic activity (28.9 ± 22.4) ($P < 0.05$), suggesting bisGMA and TEGDMA monomers played significant role in the overall cytotoxicity of photocurable systems involving HDPCs.

Significance: Cyclic acetals were capable of facilitating photo-induced free radical polymerisation reactions with relatively less cytotoxicity compared with their amine counterparts, which might realise reduced cytotoxicity of photocurable materials used for dentistry and biomaterial applications.

Keywords: Camphorquinone, co-initiators, N-Phenyl glycine, benzodioxole, piperonyl alcohol, quantum yield, absorption coefficient, molar absorptivity, MTT, cytotoxicity

1 Introduction

The use of (tertiary) amines to produce free radicals during photo-induced polymerisation of dental resin-based compsites (RBCs) and other polymeric biomedical materials offer numerous advantages: spatial and temporal control of the setting material and rapid on-demand polymerisation reaction [1, 2] . Formation of crosslinked polymer matrices occur when (di/tri-) functionalised monomers such as bisphenol-A-glycidyldimethacrylate (BisGMA), and triethylene glycol dimethacrylate (TEGDMA), and trimethylolpropane triacylate (TMPTA) are rapidly photopolymerised in the presence of a mono, binary or tertiary-based photoinitiator system. Camphorquinone, CQ (1,7,7-trimethylbicyclo [2.2.1] heptane-2,3-dione) is a photosensitiser with a visible-light absorption band ranging between 400-500 nm (λ_{max} 468 nm) [3, 4]. With the use of amine as a co-initiator, it collectively serves to as a binary photoinitiator system to instigate and promote polymerisation via bimolecular interaction involving hydrogen abstraction to generate free radicals (Figure 1).

Despite their effectiveness in generating reactive species, the biocompatibility and cytotoxicity of amines in methacrylate-based photocurable dental resins and biomaterials remains a significant concern, particularly when materials begin to leach out as a result of incomplete photocuring [5-8]. From esthetic point of view, tertiary amines are known to form by-products, during photoinduced reaction and heat, that lead to discolouration [9-12]. Recent research efforts have shifted towards investigating alternative co-initiators to improve the overall intrinsic biocompatibility of restorative and implantable materials for dental and biomedical applications, in addition to poor colour stability associated with aromatic amines as co-initiators [9].

1,3-benzodioxole (BZD; Figure 1) and its derivatives are widely found in nature, human diet and cosmetics [13-15]. They exhibit antibacterial and antioxidant properties against free radicals under oxidative stress [16-18]. Yokota *et al.,* [19], reported the use of BZD derivatives for improving the efficiency of cancer hyperthermia therapy by inhibiting thermotolerance responses of human tumour cells lines (mRNA), which has also included human colon carcinoma, nasopharynx carcinoma and human leukaemia (HL-60) cells [19, 20]. Cylic acetals have been reported to act as co-initiators in photopolymerisation of dental resins involving CQ [15, 21] Likewise, N-phenyl glycine (NPG) is an amino acid that reportedly serves as a potent substituent to conventional tertiary amines. NPG has been previously used for the synthesis of indigo dye [22], though its derivatives have been employed in photoinitiating systems involving dyes, such as xanthene [23] and azomethine [24] for free radical photopolymerisation. NPG is considered to be non-allergic and biologically less damaging than amines. Glycine derivatives have also been proposed as co-initiators for polymeric dental formulations. More importantly NPG has shown to promote polymerisation even in the presence of

water, an attribute that is particularly favourable for bonding in aqueous conditions, which are prevalent in restorative dentistry and biomaterials field [26].

Consequently, the aims of this study were to, 1) assess NPG, BZD and its alcohol derivative as co-initiators in a CQ-based photoinitiating system, by understanding the effects of co-initiator concentration on DC (%) and the quantum yield of conversion of CQ molecules as a function of absorbed photons, and 2) evaluate cytotoxicity of NPG and cyclic acetals with respect to conventional amines, by assessing metabolic activity of HDPCs.

2 Materials and Methods

Unless specified, all materials were supplied by Sigma-Aldrich, Gillingham, UK.

2.1 Model resin system

For this study, a 1:1 mass ratio of bisGMA/TEGDMA was used as the resin model system. Table 1 summarises the model resin formulations with varying concentrations of CQ and co-initiators (Figure 1), used in this study.

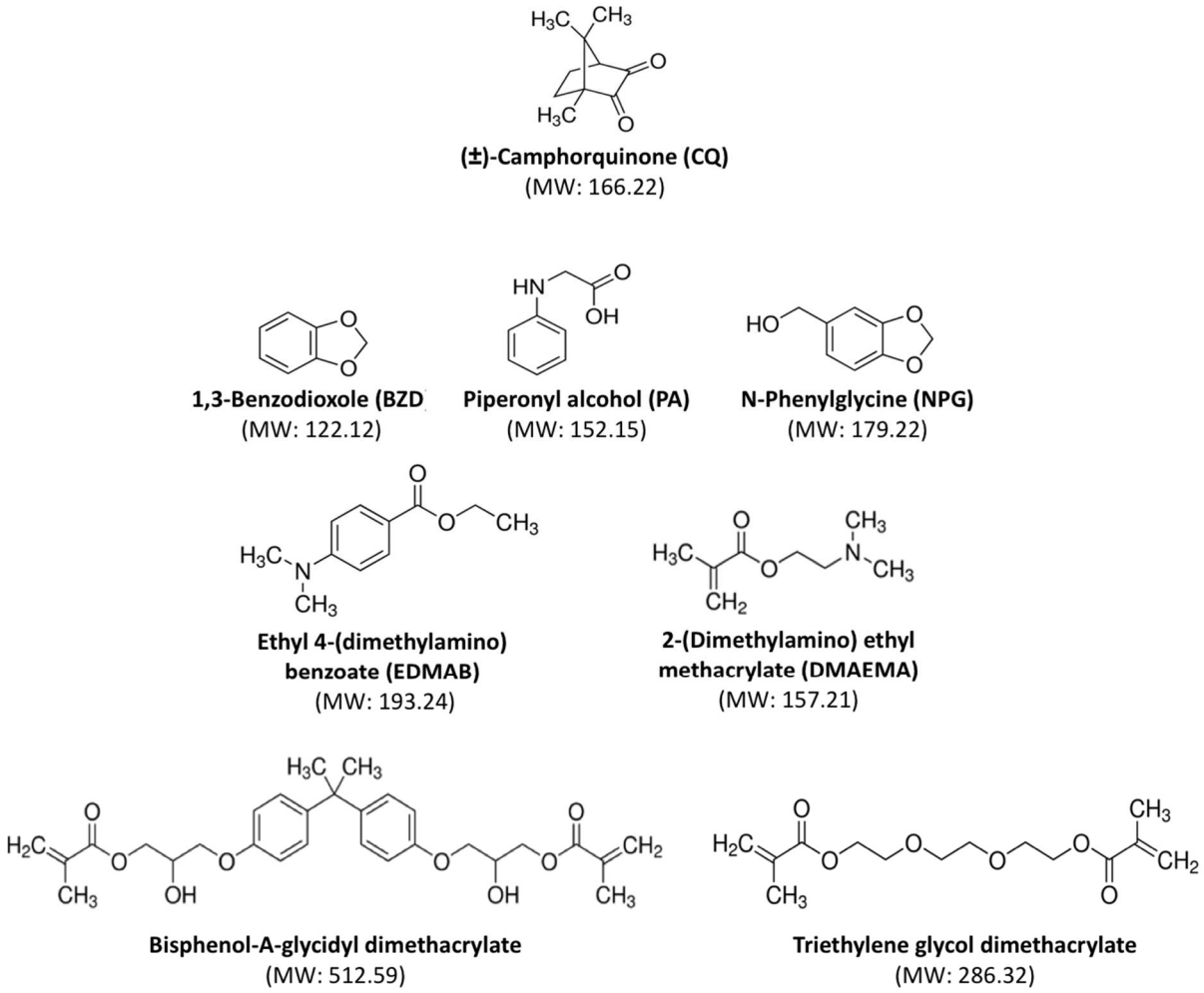

Figure 1: *Chemical structures of proposed alternative co-initiators, conventional (tertiary) amines and CQ.*

Table 1: *Summary of CQ to co-initiator concentration ratios studied in a BisGMA/TEGDMA (50/50 wt.%) resin model system.*

CQ (mol %)	***Co-Initiators (mol %)***				
	DMAEMA	**EDMAB**	**NPG**	**BZD**	**PA**
0.5 (Low), 1.0 (Intermediate), 1.5 (High)	0	0	0	0	0
	0.5	0.5	0.5	0.5	0.5
	1.0	1.0	1.0	1.0	1.0
	1.5	1.5	1.5	1.5	1.5
	2.0	2.0	2.0	2.0	2.0
	3.0	3.0	3.0	3.0	3.0
	4.0	4.0	4.0	4.0	4.0
	6.0	-	-	6.0	6.0

2.2 Absorbance

UV-Vis absorbance by CQ and co-initiators were determined using a miniature spectrophotometer (USB4000; Ocean Optics, Florida, USA). A 400 µm optical fibre, coupled with a cosine corrector (CC3-UV; diameter 3.9 mm) was used to measure the spectral absorbance of photoinitiators in a 2 mm pathlength plastic cuvette (UVette, Eppendorf, Germany) and a 1.8 x 1.8 mm square aperture (Figure 2a). Prior to all experiments, the spectrophotometer setup was calibrated using a calibration lamp (DH-2000-CAL; Ocean Optics, Ostfildern, Germany) [27]. For static absorbance measurements, 150 µL of each co-initiator (1.0 mol %) (n = 3) dissolved in methanol (VWR International, UK) was aliquoted into a new cuvette and placed inside the sample holder. The DH-2000-CAL light source was used to determine the absorbance of each co-initiator in the UV-Visible (200-800 nm) range.

2.2.1 Molar Extinction Coefficient

The molar extinction coefficient or molar absorptivity, ε (cm^{-1}/ $mol.L^{-1}$) of CQ was determined by calculating the absorption coefficient, μ_a of CQ ($mol.L^{-1}$) dissolved in the resin model system at varying concentrations, using the experimental setup depicted in Figure 2a and the DH-2000-CAL light source.

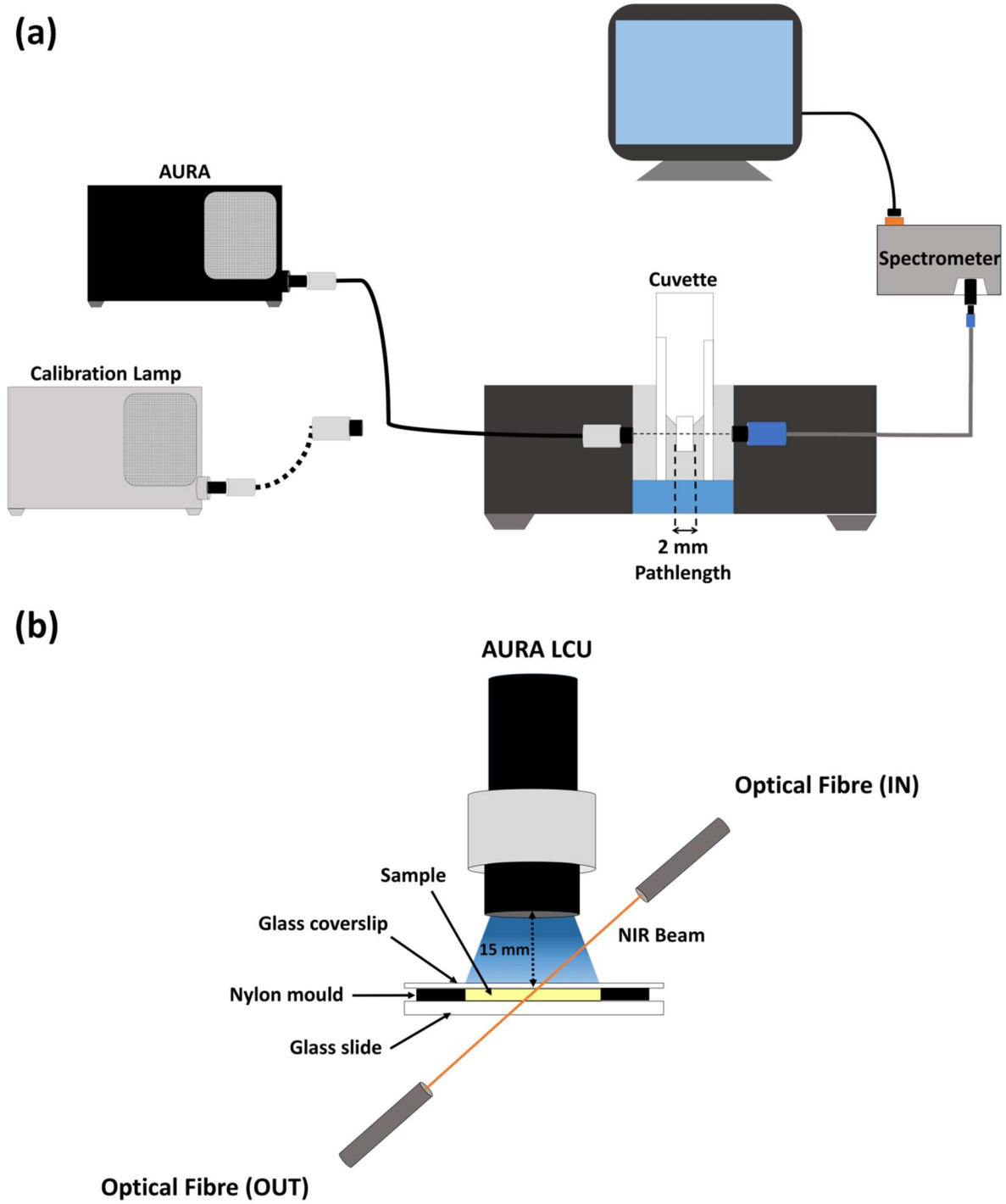

Figure 2: *Experimental setup for real-time absorption measurements using spectrophotometer (a) coupled with either DH-2000-CAL or a light curing unit (AURA). Real-time photopolymerisation and rates of reaction measurements using FT-NIRS (b) in transmission mode through a 2 mm specimen mould.*

2.3 DC and rate of photopolymerisation

To measure polymerisation rate and DC (%), 0.22 – 0.24 g of each formulation was carefully transferred to fill a black Nylon mould (12 mm diameter, 2 mm thickness) with 1.1 mm thick microscope glass slide beneath. To reduce oxygen accessing free radicals, the resin mixture samples

were covered with a glass cover slip (0.1 mm) prior to light irradiation and polymerisation. Using the experimental arrangement in Figure 2b, specimens were irradiated at 15 mm distance using a AURA light engine® (Lumencor®, Oregon, USA) with an homogeneous beam profile [28]. A consistent irradiance of 425.8 ± 0.06 mW/cm^2 at 470 nm was delivered throughout the photopolymerisation studies for 300 s (n = 3). It is worth noting that the use of high co-initiator concentration (i.e., 6 mol %), was to explore if concentration had an effect on the overall efficiency of photoinitiation system. The recommended co-initiator concentrations are well below that and has been discussed in Section 4 and 5 accordingly.

DC (%) and C=C double bond conversion of each formulation were determined using real-time Fourier transform near infrared spectroscopy (FT-NIRS; Figure 2b) (Nicolet 6700 FT-IR, Thermo Scientific, Hemel Hampstead, UK) in transmission mode by monitoring the peak height at 6164 cm^{-1}, which corresponded to the decay of the vinyl–CH_2 absorbance. In order to observe maximum DC during illumination, polymer conversion was monitored for 300 s (n = 3), with data acquisition every 100 ms. Rates of polymerisation were determined by calculating the first derivative of DC (%) acquired with respect to time during photopolymerisation. A moving-average smoothing technique was applied to rate traces, to reduce background noise.

2.3.1 Irradiance measurement

Prior to polymerisation and DC (%), the irradiance received by the test piece from the AURA LCU was measured using the UV-Vis spectrophotometer setup depicted in Figure 1a (without the cuvette) (Section 2.2), whilst accounting for the 15 mm distance between light tip and specimen surface and attenuation through glass-resin interfaces, involving FT-NIRS (Figure 2b). Equally, transmittance of light through an empty sample holder (with glass slide beneath and cover slip above), was substracted (as background) from measurements to normalise the data. Similar configuration was used, except for replacing AURA with a UV LCU – Omnicure series 1000 (Lumen Dynamics, Ontario, Canada), employed to measure received irradiance and real-time photopolymerisation of neat model resin system. At 15 mm distance from specimen surface, the absolute irradiance of Omincure LCU was 68.2 ± 0.7 (mW/cm^2) (λ_{max} = 314 nm), 79.5 ± 0.1 (mW/cm^2) (λ_{max} = 334 nm), 1406.3 ± 3.1 (mW/cm^2) (λ_{max} = 366 nm), 580.6 ± 1.0 (mW/cm^2) (λ_{max} = 405 nm) and 1137.4 ± 1.4 (mW/cm^2) (λ_{max} = 436 nm) (Section 3.1; Figure 3b).

2.4 Quantum Yield, ϕ

2.4.1 Photon absorption and CQ conversion

To measure the quantum yield of conversion of CQ as a function of photon absorption in the presence of different co-initiators, real-time absorption decay of CQ with data acquisition every 500

ms for 600 s (n = 3) was measured (Figure 2a) with the AURA light source calibrated to deliver similar irradiance (428.1 ± 0.1 mW/cm^2), used for photopolymerisation measurement, at 470 nm. Since the specimen thickness affects the CQ consumption, a 2 mm pathlength cuvette (UVette, Eppendorf, Hamburg, Germany) was used to correlate ϕ with photopolymerisation measurements obtained from FT-NIRS.

Absorption coefficient, μ_a as a function of CQ molar concentration was determined using Equation 1. Where, A(λ) is the measured absorbance (decay) at 470 nm with respect to time (t), and d the specimen thickness (0.2 cm) [29].

$$\mu_a = A(\lambda)(\ln 10)/d \quad (1)$$

Since absorption coefficient decay with illumination time can be modelled exponentially, the time constant fitting parameter, τ was calculated empirically by applying a non-linear fitting curve using Equation 2 [29].

$$\mu_a(470,\ t) = \mu_{a0}(470\ nm)\exp(-\frac{t}{\tau}) \quad (2)$$

Where μ_{a0} (λ), is the initial absorption coefficient at 470 nm (t = 0). Depending on the type and molar concentration of each co-initiator, the absorption decay was modelled as mono or bi-exponential function to determine τ, using fitting curve tool (MATLAB R2016b; MathWorks, USA). For bi-exponential absorption models, only the first phase of the exponential decay was used to calculate the time constant, since the second phase followed a linear trace.

The ϕ conversion of CQ is defined as the ratio of the number of converted CQ molecules to the number of photons absorbed, (Equation 3) [29].

$$\Phi = \frac{\sum_0^t \sum_{\lambda_1}^{\lambda_2} Q(\lambda, t')\Delta\lambda\Delta t'}{\left(\frac{\mu_{a0,\lambda}}{\varepsilon_\lambda \ln 10}\right)\left(\frac{N}{\text{litre}}\right)\exp\left(-\frac{E_{total}t}{H_{threshold}}\right)} = \frac{A_{photon}(t)}{C(t)} \quad (3)$$

Where, Q (λ, t) is the number of absorbed photons by CQ (Vol/s). The accumulated number of photons, $A_{photons}$ (t), corresponds to the sum of Q (λ, t) at 470 nm, when t = 0 to t = t (600 s). Similarly, C (t) corresponds to the concentration of the remaining CQ as a function of curing time. Since CQ molecules are being converted into radicals, the loss of absorption properties corresponds to its conversion. ε_λ is the molar extinction coefficient at 470 nm, N refers to the Avagadro's constant and E_{total} is the total applied irradiance (428.1 ± 0.1 mW/cm^2).

For each formulation, ϕ of CQ conversion was obtained by plotting C versus A_{photon}, the slope of which corresponds to CQ consumption per absorbed photon [29].

2.5 Cytotoxicity

2.5.1 Cell culture

Following ethical approval from BBC CLRN RM&G consortium office, human dental pulp cells (HDPCs) were isolated from a caries free healthy patient via an established explant procedure [30]. HDPCs were then cultured in a T75 (75 cm^2) flask within Dulbecco's Modified Eagle's Medium (DMEM) - High glucose (Biosera, Heathfield, UK), supplemented with 10 % foetal bovine serum (FBS), penicillin-streptomycin (100 U/mL – 100 µg/mL) and L-Glutamine (100 µg/mL). Cell cultures were incubated at 37°C in a 5 % CO_2 humidified atmosphere with media change every 48 h. The flasks were sub-cultured, upon reaching almost full confluency, every 72 h to 96 h using standard trypsin/EDTA solution protocol [31]. Based on previous studies [32], and to avoid HDPCs differentiating, only cells from the 2-4th passages were used for present work.

2.5.2 Polymerised resin eluates

To conduct cell studies on released eluates, resin model formulations each containing CQ (1.0 mol %) and a co-initiator at its 'optimal' concentration in terms of DC (%) and quantum yield of conversion of CQ (CQ/EDMAB: 1:4 mol %, CQ/DMAEMA: 1:2 mol %, CQ:BZD: 1:4 mol %, CQ/PA: 1:4 mol %, CQ/NPG: 1:2 mol %), were prepared. For each formulation, 12 × 2 mm specimens (n = 3) were prepared by photocuring using the irradiance and experimental setup described in Section 2.3, followed by aseptic cotton swabbing with 70 % ethanol. To test cytotoxicity of the neat model resin (i.e. without CQ or co-initiator), specimens were photopolymerised using Omnicure series 1000 for 300 s, involving experimental setup and irradiance measurement described in Section 2.3. It is proposed that photolysis of the model resin system by UV light would have generated free radicals and initiated photopolymerisation. BisGMA is more susceptible to intense UV irradiation due to absorption by phenyl groups (conjugated systems) [33-35]. Specimens were then incubated in a sterile 24 well plate (Nunclon Delta surface, ThermoFisher Scientific, Denmark) within serum-free DMEM at 37°C with 5 % CO_2 supply. For each specimen, the volume of medium was adjusted to give an extraction ratio of 1 mL/3 cm^2 surface area, in accordance with ISO 10993-12:2012 [36]. Specimens were incubated separately for 24 hours and 7 days to obtain two different released eluate concentrations. During the extraction process, specimens were gently agitated, every day for ~30 minutes, using an orbital shaker (Luckham R100/TW, England, UK). The present cell work is based on the 7-day old eluates, as preliminary studies involving 24 h-old media eluates exhibited no significant biological effects.

2.5.3 Metabolic activity

Cells were seeded on sterile 96 flat bottom black well plates (4titude, Surrey, UK) with 5,000 cells density within each well (n = 3) per plate. Each experiment was performed in triplicate per

treatment group. Cells were then incubated with supplemented DMEM for 24 h to allow cellular adhesion to the cultureware. After 24 h, selected cultures were treated with collected eulates and incubated for further 24 h. Prior to incubation, collected eluates were diluted to 1:3 ratio with fresh media supplemented with 10 % FBS. The FBS amount was adjusted for the total volume of 150 µL per well. To assess cellular metabolic activity after 48 h, the initial media was replaced with supplemented phenol free DMEM - high glucose (Gibco, Life technologies, UK), with 10 % 3-(4,5-Dimethyl thiazole-2-yl)-2,5-di-phenyl tetrazolium bromide (MTT) stock solution (5 mg/mL in PBS) [31], and left to incubate for 4 h in a humidified atmosphere at 37°C with 5 % CO_2 supply. The use of clear media eliminated interference of phenol red during absorption measurements (in accordance with ISO 10993-5:2009) [36, 37]. Following incubation, media along with MTT solution was removed and dimethyl sulfoxide (DMSO) (Fisher Scientific, UK) was added to each well to dissolve formazan crystals. Culture plates were placed on an orbital shaker, under low speed control, for ~ 5 minutes to allow complete dissolution, before reading absorbance at 570 nm using Spark plate reader (Tecan Group ltd., Mannedorf, Switzerland). Background absorbance was calculated through the use of empty wells containing equivalent amount (50 µL) of DMSO. An average background absorbance value was subtracted from obtained results to normalise the data.

2.5.4 Statistical analysis

One-way analysis of variance (ANOVA) and post-hoc Tukey's tests, at 95 % confidence interval ($n = 6$), were performed to determine significance ($p < 0.05$) between treated and untreated groups in terms of metabolic activity involving HDPCs. Separate one-way ANOVAs and post-hoc Tukey's tests were carried out to compare DC (%) (final values), Rp_{max} (s^{-1}), τ (s) and ϕ, based on co-initiator concentration (0.5 – 6.0 mol %) of an individual co-initiator at a given CQ concentration (0.5, 1.0, 1.5 mol %) in a model resin system. Significant confidence intervals are indicated in graphs (* $p < 0.05$, ** $p < 0.01$, *** $p < 0.001$).

3 Results

3.1 Absorbance and molar absorptivity, ε

Figure 3a shows the static absorbances of CQ and co-intiators dissolved in methanol. CQ showed strong absorption within 400-500 nm band with λ_{max} at 469 ± 2 nm. Likewise, NPG showed broad absorption spectrum within the UV-visible region, with its absorption shoulder overlapping with that of CQ around 450-495 nm. Figure 3b, depicts relative irradiances of both the AURA and Omincure light sources.

The molar absorptivity, ε (cm^{-1}/ $mol.L^{-1}$) of CQ was determined by calculating the absorption coefficient, μ_a of CQ ($mol.L^{-1}$) at different concentration using DH-2000-CAL. Figure 3c, illustrates the slope of the regression line and the relationship between μ_a and CQ concentration ($\mu_a = (\ln 10)\varepsilon_{470}C$). The molar absorptivity of CQ at 470 nm was calculated to be 42.46 ± 2 $cm^{-1}/(mol.L^{-1})$, which correlates well with published findings [29, 38].

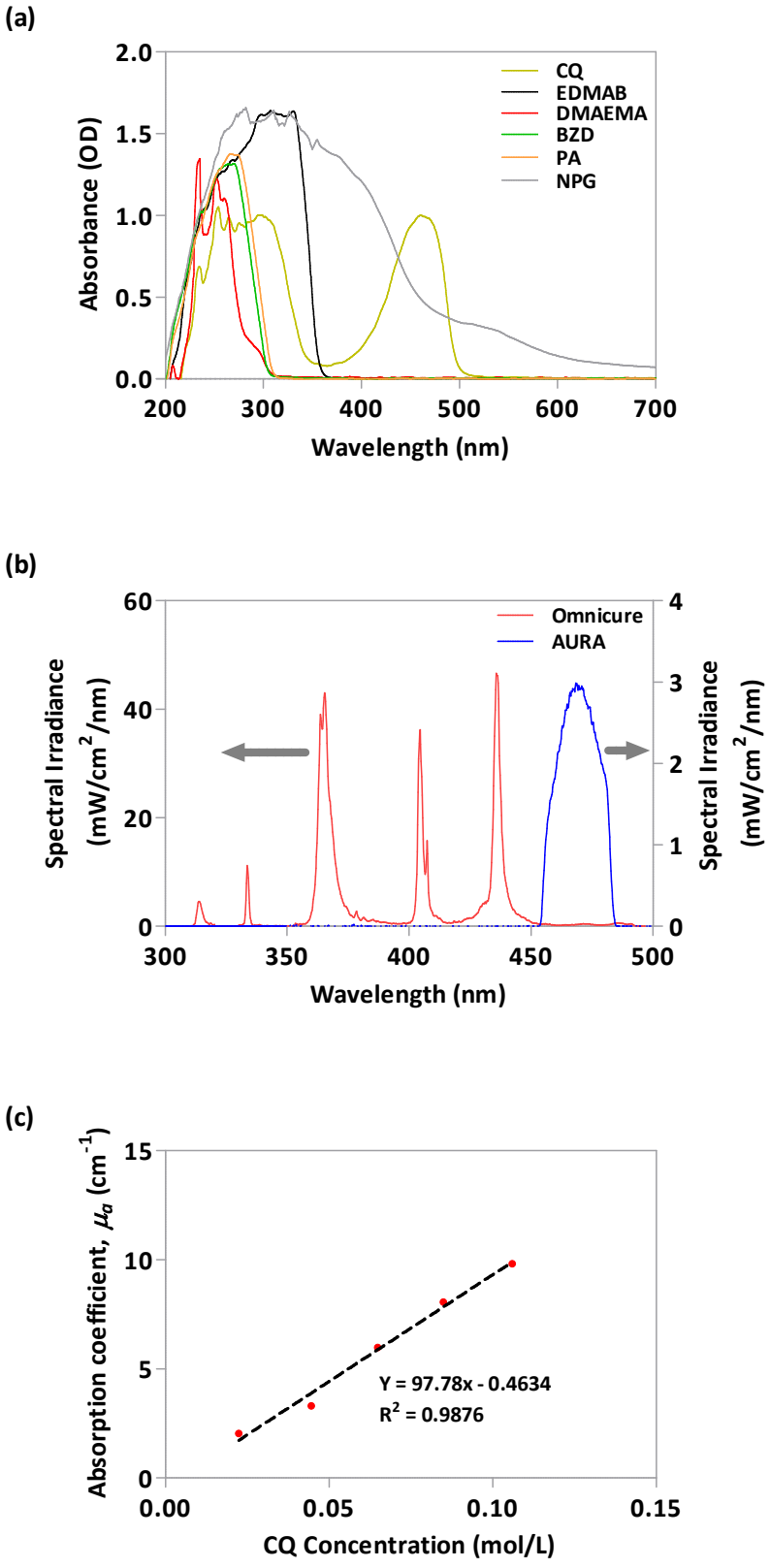

***Figure 3**: Static absorbances of (a) CQ and co-initiators (1.0 mol %) dissolved in methanol. (b) - Absolute irradiances of Omnicure (Left y-axis) and AURA LCU (Right y-axis). (c) Absorption coefficient, μ_a at 470 nm as a function of CQ concentration (mol.L^{-1}) in a 1:1 wt.% resin model system. Using the relationship between the two ($\mu_a = (\ln 10)\varepsilon 470C$), the molar absorptivity of CQ at 470 nm was calculated to be 42.46 ± 2 cm^{-1}/(mol.L^{-1}).*

3.2 DC and rate of photopolymerisation

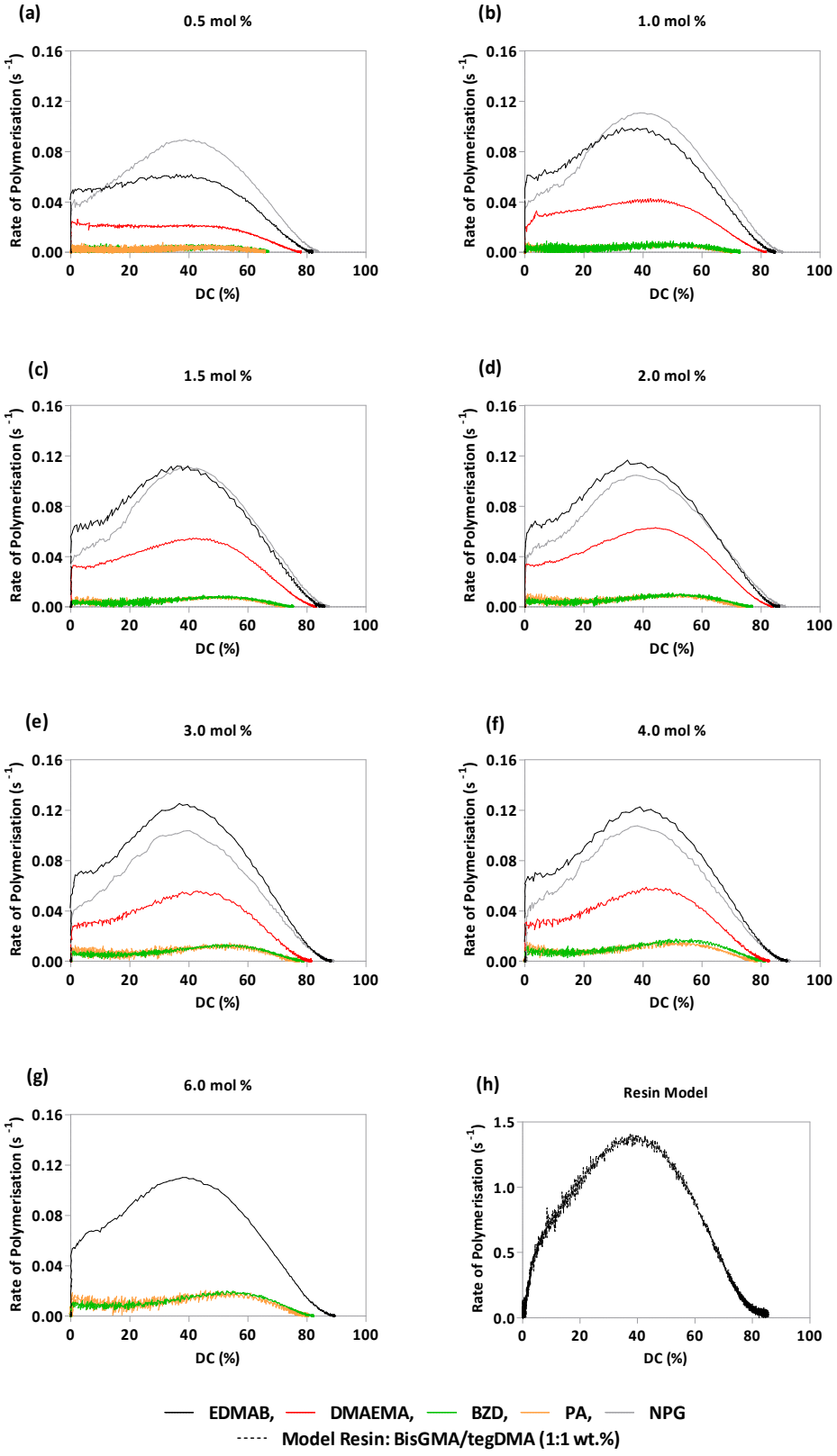

Figure 4: *Mean DC (%) (x-axis) and rate of photopolymerisation (y-axis) of resin model system (BisGMA/TEGDMA, 1:1 wt.%) photopolymerised in the presence of 1.0 mol % CQ and different co-initiators at varying concentrations (0.50 - 6.0 mol %) under 425.8 ± 0.06 mW/cm² for 300 s with data acquisition every 0.1 s.*

DC and rate of photopolymerisation of the resin model system generally increased sequentially with co-initiator concentration, irrespective of CQ concentrations (0.50 mol %; Supplementary 1A, 1.0 mol %; Figure 4, and 1.5 mol %; Supplementary 1A) in the resin mixture. Figure 4a-g shows real-time photopolymerisation of the resin model system containing 1.0 mol % CQ with various co-initiators at different concentrations (0.5 – 6.0 mol %). The extent of polymerisation ranged from 82.6 ± 0.7 (%) and 82.0 ± 0.3 (%) for respective DMAEMA- (4.0 mol %) and BZD-based (6.0 mol %) formulations, to 80.3 ± 0.0 (%) for PA at 6.0 mol % concentration with respect to 1.0 mol % CQ in the model resin system. Likewise, NPG and EDMAB-based formulations exhibited 89.6 ± 0.2 (%) and 89.3 ± 0.2 (%) at respective 4.0 and 6.0 molar equivalent concentrations.

Figure 4h corresponds to the photopolymerisation of the neat resin model (without CQ or binary photoinitiating system), under a UV LCU (Omnicure series 1000). Real-time DC of neat resin model was measured to be 85.3 ± 0.3 %. Equally, Figure 5 summarises Rp_{max} (s^{-1}) and associated DC (%) obtained with various co-initiators at varying concentrations involving 1.0 mol % CQ. Both variables generally increased ($p < 0.05$, indicated by asterisks) following the subsequent molar equivalent increase in co-initiator concentration, when compared with 0.5 mol % co-initiator of the same type. Similar trends were observed for both parameters for formulations containing 0.5 mol % and 1.50 mol % CQ (Supplementary 1A). However, variation in DC (%) at Rp_{max} (s^{-1}) were not statistically significant ($p > 0.05$) at 1.50 mol % CQ concentration, when compared via post-hoc Tukey's test following one-way ANOVA.

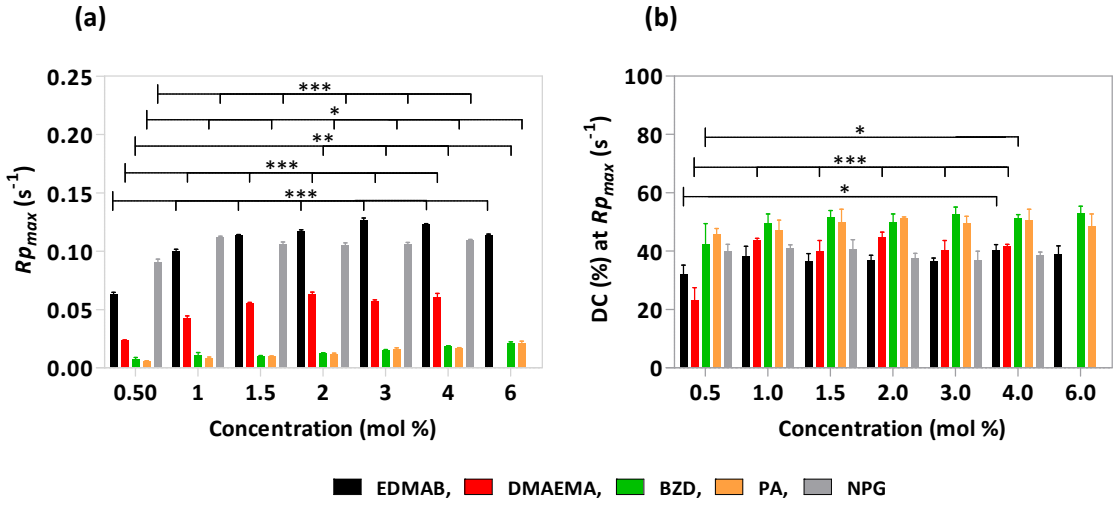

***Figure 5**: Summary of (a) Rp_{max} (s^{-1}), and (b) DC (%) at Rp_{max} (s^{-1}) of resin model system involving, CQ (1.0 mol %) with different co-initiators at varying molar concentrations (0.5 - 6.0 mol %) in a resin model system. Asterisks (* $p < 0.05$, ** $p < 0.01$, *** $p < 0.001$) indicate statistically significant differences, when compared with 0.50 mol % concentration involving each respective co-initiator type. Based on Tukey's post-hoc test following one-way ANOVA.*

The use of NPG as a co-initiator resulted in increased in final DC (%) compared with that of EDMAB at low concentrations (0.5 – 2.0 mol %; Figure 4a-g). Equally, no significant improvement ($p > 0.05$) in DC (%) at Rp_{max} (s^{-1}) was observed beyond 1.5 mol % NPG, with associated DC (%) were comparatively similar to that of EDMAB beyond 2.0 mol %. The difference between the two co-initiators, was most apparent in formulations containing low CQ concentration (0.5 mol %; Supplementary 1A), and became less significant at formulations containing high CQ concentration (1.5 mol %; Supplementary 1A). In the case of reaction rates involving 1.0 mol % CQ concentration, Rp_{max} (s^{-1}) remained somewhat constant at NPG concentrations > 2 mol % (Figure 5a). Nonetheless, increase in Rp_{max} (s^{-1}) following subsequent increase in mol % NPG was statistically significant when compared with 0.50 mol % NPG via post-hoc test following one-way ANOVA (Figure 5a).

3.3 Absorption Coefficient, μa (cm^{-1}) and Quantum yield of conversion of CQ

Figure 6 illustrates change in absorption coeffiecient, μa (cm^{-1}) of CQ (1.0 mol %) in the presence of different co-initiators at varying concentrations, in the resin model system (BisGMA/TEGDMA, 1:1 wt.%).

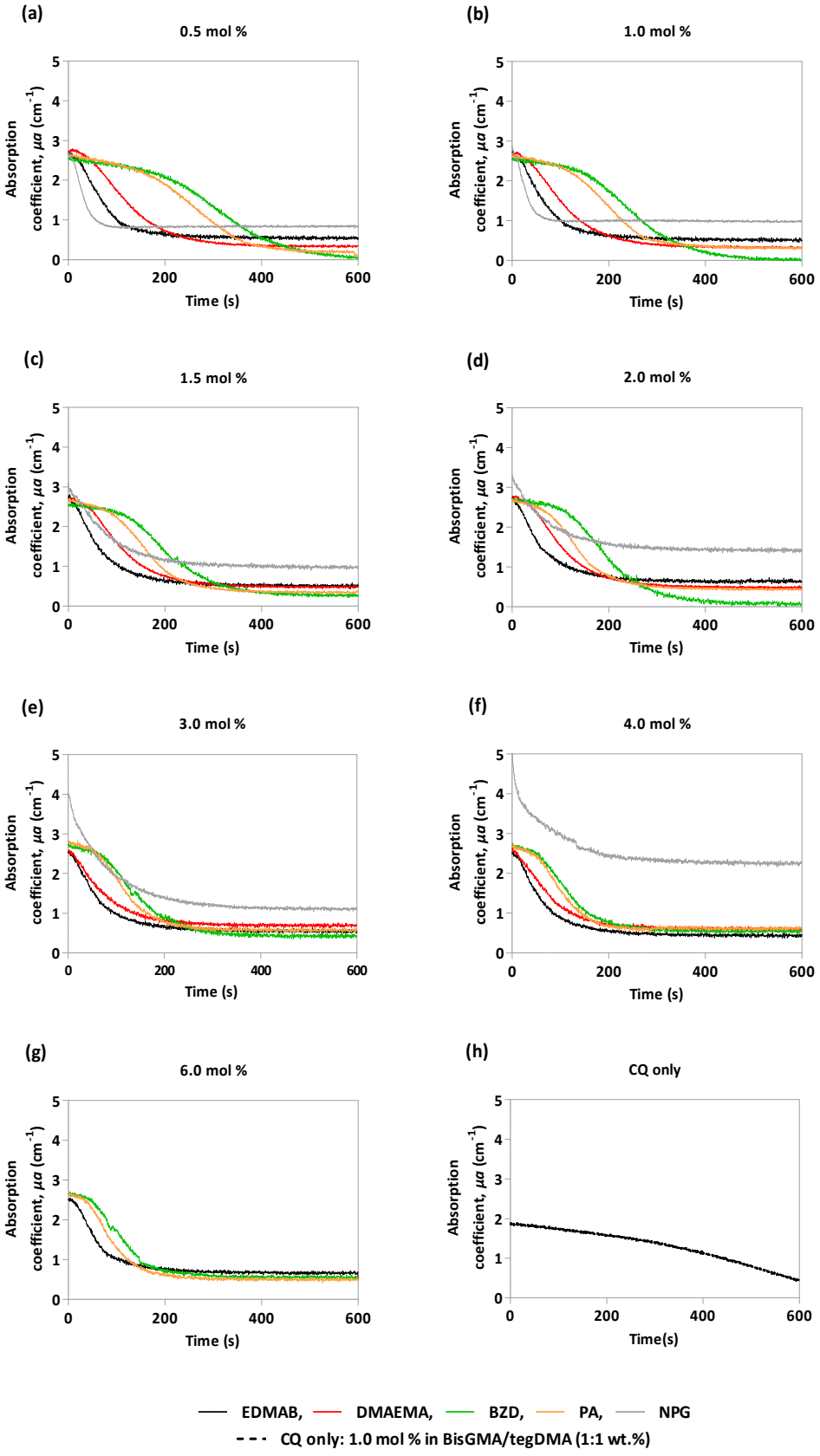

Figure 6: *Mean absorption coefficient μa, of CQ (1.0 mol %) alone and in the presence of co-initiators at varying concentrations (0.5 - 6.0 mol %), under 428.1 ± 0.1 mW/cm² for 600 s with data acquisition every 0.5 s.*

With successive increase in molar concentration in the resin model, the use of cyclic acetals steadily improved the absorption decay of CQ, as evidenced by decrease in τ, (Figure 7a below), when compared with formulations with CQ alone and concentrations containing 0.5 mol % co-initiator ($p < 0.05$). The use of PA resulted in slightly better ϕ (and τ) values when compared with BZD (Figure 7). For 1.0 mol % CQ, the use of NPG as a co-initiator only resulted in small improvement of CQ absorption decay (Figure 6a-g), with τ values (Figure 7a) comparable to that of tertiary amines. Equally, ϕ increased significantly ($p < 0.05$) at lower concentrations before declining at higher molar equivalent concentrations. The decline was statistically significant at 1.5 to 3 mol %, ($p < 0.05$), when compared with 0.5 mol % NPG as a co-initiator in the 1.0 mol % CQ resin model via post-hoc test following one-way ANOVA (Figure 7b).

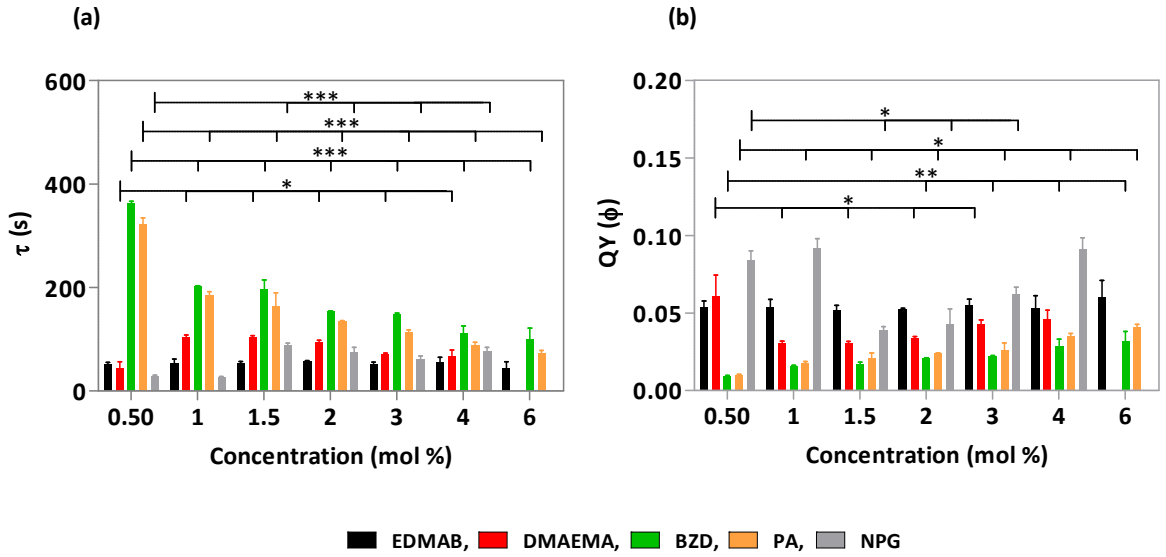

***Figure 7**: (a) Mean τ and ϕ (b) of CQ (1.0 mol %) in the presence of alternative co-initiators at varying concentrations (0.50 - 6.0 mol %). Parameters were determined by an established calculation principle devised by Chen et al., [29]. Asterisks (* $p < 0.05$, ** $p < 0.01$, *** $p < 0.001$) indicate statistically significant differences, when compared with 0.50 mol % concentration involving each respective co-initiator type. Based on Tukey's post-hoc test following one-way ANOVA.*

3.4 Cell assays

Figure 8 shows the relative metabolic activity of HDPCs treated with 7-day old eluates of the photocured neat resin model photopolymerised using various binary photoinitiating systems at optimal concentrations based on DC and ϕ values. The MTT assay showed a relative reduction of ~42 and 43 % in metabolic activity of HDPCs following 24 h exposure to formulation eluates of resin model photocured using BZD and PA as co-initiators, respectively. Likewise, treatment with EDMAB and DMAEMA-based eluate reduced HDPCs metabolic activity by ~48 and 40 %, respectively.

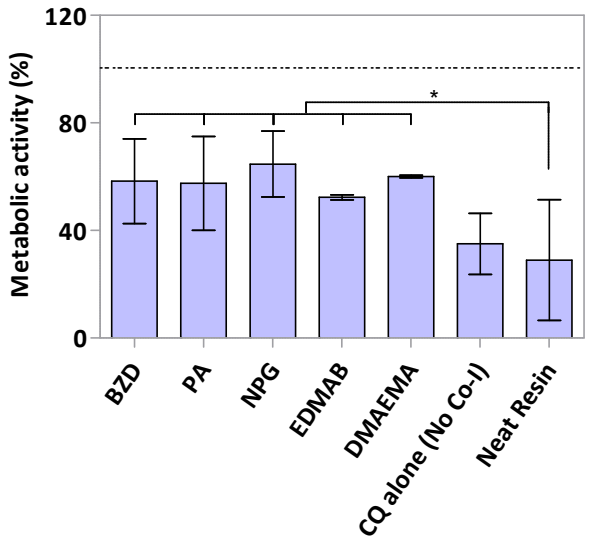

Figure 8: *MTT assay to assess metabolic activity of HDPCs treated with 7-day old formulation eluates for 24 h, of photocured neat resin model, and resin mixture containing CQ alone (No co-initiator) or with various co-initiators at optimal concentrations. Dashed line correspond to mean value (%) of untreated group (Control). Bars represent mean and bars signify standard deviation (SD) of each treatment group with respect to control. Asterisks (* $p < 0.05$) indicate statistically significant differences between groups, via post-hoc test following one-way ANOVA.*

The reduction of ~35 % in metablic activity was observed for groups treated with NPG-based collected eluate, and was statistically significant ($p < 0.05$) when compared with control via post-hoc Tukey's test following one-way ANOVA. Treatment with CQ-only, and the neat resin model-based eluate led to highest reduction ($p < 0.05$) of ~65 and 71 %, when compared with untreated group (Control) at mean values via post-hoc test following one-way ANOVA.

4 Discussion

4.1 DC and rate of photopolymerisation

CQ itself can initiate photopolymerisation reactions via carbonyl radicals that are formed by homolytic cleavage of the carbon-carbon bond between the two carbonyl groups. However, (tertiary) amines are commonly used in dental RBCs, including resin-based biomaterials, to facilitate appropriate reaction rates by utilising α-aminolkyl radicals produced via a hydrogen abstraction process. These radicals are highly effective and predominantly responsible for initiating the polymerisation reaction by reducing curing times significantly [39]. Dental RBCs, adhesives and bone cements undergo either chemical or dual (photo-activated)/cationic free radical curing mechanisms. Accelerators such as diphenyliodonium hexaflurophosphate are incorporated to improve efficiency, though it use may be valid for CQ/DMAEMA systems only [40]. A reduction in curing time is considered beneficial particularly during clinical applications involving restorative dentistry and bone

augmentation procedures. Whereby, self- or dual-cured materials offer a limited window for manipulation, post mixing. In addition, heat generated during polymerisation reactions could be detrimental to local cellular tissues, especially during *in situ* polymerisation. Likewise, operating at the UV range limits the use of such systems for curing thin layers only [41], and shorter wavelengths may induce greater phototoxicity.

The current study investigated cyclic acetals and NPG, as these compounds are reportedly capable of acting as co-initiators in a Type II diketone-amine photointiator systems [13, 15, 21, **Error! Hyperlink reference not valid.**, 26, 42-45]. To compare their viability as co-initiators in dental adhesives, RBCs and/or bone augmentation materials; conventional amines namely, DMAEMA and EDMAB were used as comparison examples, since their reactivity with CQ are well-documented [38, 39, 46, 47]. The present work only demonstrates data involving 1.0 mol % CQ. Supplementary 1A provides data on the resin model system involving 0.5 and 1.5 mol % CQ formulations. It is worth noting that TEGDMA monomer used in present study, contained hydroquinone monomethylether (MEHQ) (80-120 ppm) to avoid premature polymerisation. Alhough present in minute amount, the inhibitory effects of MEHQ on polymerisation involving cylic acetals and NPG should be taken into account, and yet to be elucidated.

Photocuring efficiency is dependent upon the type and the steric structure of the derived radical [48]. Both amines, despite being structurally different (DMAEMA, aliphatic; EDMAB, aromatic) demonstrated effective photocuring at low (0.5 mol %), intermediate (1.0 mol %) and high (1.5 mol %) CQ concentrations. Irrespective of molecular structural differences, DC of the resin model system at $Rp_{max}(s^{-1})$ (Figure 5b), generally increased with amine concentration. The use of EDMAB as a reducing agent resulted in greater $Rp_{max}(s^{-1})$ and associated DC (%) (Figure 5), when compared with DMAEMA. This is due to the higher efficiency and reactivity of aromatic amine-derived radicals in withdrawing character of the (methyl) groups attached in the β-position of the N atom [47, 48].

However, $Rp_{max}(s^{-1})$ of CQ/EDMAB-based photoinitiating systems varied across all three CQ concentrations. For 1.0 mol % CQ blend, the highest $Rp_{max}(s^{-1})$ (Figure 5a) was observed at relative 3.0 mol % EDMAB, beyond which the value began to decrease slightly when the relative EDMAB molar concentrations was increased. The associated DC (%) also began to level out at or beyond 3 mol % (Figures 4a-g and Figure 5b), with little or no significant improvement in DC across all three CQ blends (0.5 and 1.5 mol %; Supplementary 1A). Fluctuations in DC (%) are likely attributed to time to reach Rp_{max} (s^{-1}) due to poor structural stability, caused by the conjugated aromatic ring of EDMAB [49]. A relatively low increase in associated DC (%) at higher molar concentrations of EDMAB (Figure 5b) might be attributed to the early onset of vitrification due to rapid change in the viscosity of the resin model, since the effective diffusion of amine-derived radicals through the rapidly increasing crosslink density

becomes restricted. An increased number of CQ electrons return to their ground state, which reduces yield efficiency observed herein due to an increase in the time constant, τ which corresponds to 1/e decay of CQ absorption (Figure 7a).

For the DMAEMA-based photoinitiating system, DC improved with higher DMAEMA concentrations until ~1.5 mol % and began to decline beyond 2 molar equivalent concentration (%) to CQ. This included post-irradiation DC (%) (Figure 4) and DC (%) at Rp_{max} (s^{-1}) (Figure 5b). Such behaviour was observed across all three CQ concentrations (0.5 & 1.5 mol %; Supplementary 1A), and in line with published data [50]. The retardant behaviour of DMAEMA is likely to be attributed to the methacrylate-bound group, which has the capacity to co-polymerise with the monomeric matrix and could potentially limit the propagation step [50] to promote the early onset of vitrification, as evidenced by decline both in Rp_{max} (s^{-1}) and associated DC (%) beyond 2 mol % (Figure 5).

When compared with EDMAB, little or no improvement in DC values of NPG-based systems beyond 1.5-2 mol % might be partially associated to the lack of excited CQ species and/or their accessibility to form a charge transfer complex (CTC) and produce radicals, particularly at low CQ concentration (0.5 mol %; Supplementary 1A). A more plausible explanation may be the competitive light absorption behaviour of NPG. Figure 3a shows the absorption spectrum of NPG overlapping with that of CQ (450-495 nm). Zhang *et al*., [45], reported photolysis of NPG at 392 nm, whereby the absorption at λ_{max} reduced with simultaneous increase in absorption at 280 nm due to the formation of N-methylaniline, and as a result of sequential cleavage of the C-COOH bond in NPG. This also serves to suggest that NPG may be capable of acting as a Type I photoinitiator. Kucybaa *et al*., [**Error! Hyperlink reference not valid.**], reported similar findings when a mixture of CQ/NPG (10:1 wt.%) was irradiated at 488 nm using a 420 mW/cm^2 light source. The authors reported a decrease in NPG absorption whereas, CQ absorption almost remained unchanged. Besides the unusally high CQ absorption coefficients (Figure 6) at 470 nm (beyond 1:1 mol % CQ/NPG), the current investigation did not observe any apparent changes in absorption at UV-visible region. This includes a resin system without CQ, whereby no curing was observed by NPG alone. The competing light effect induced by NPG was further observed, by increased τ for CQ absorption decay (Figure 7a), following the subsequent molar increase of NPG content in the resin mixture (Section 4.2). Competing light effects may pose issues in delivering an adequate amount of light for deeper curing of thick specimens, particulary composites. Likewise, the formation of photolysis products depends on many factors such as loss in efficiency from the excited singlet state to the converted radical species. For example, the excited singlet state of CQ/amine systems may return to its ground state without entering the exciplex state via intersystem crossing. Likewise, if the triplet state CQ is unable to abstract a proton, it may return to its ground state. Other factors include proton transfer back to the co-initiator (amine) or

solvent following abstraction and/or the formation of CQ•H_2 alcohol and a CQ molecule by two CQ•H radicals [29]. Beside using higher curing irradiance, another method to reduce rate-limiting factors is to enhance the proton abstraction process by increasing co-initiator concentration, and the current investigation attempted to explore such an approach. Overall, an increase in co-initiator concentrations improved post-irradiation DC (%). However, it did not lead to the total consumption (conversion) of CQ molecules, which is likely due to the intrinsic structure (an unbleachable β-carbonyl chromophore) and relatively low molar absorptivity, ε, of CQ when compared with Type I photosensitisers [51].

4.2 Absorption coefficient, μa (cm^{-1}) and Quantum yield of conversion of CQ

The use of NPG as a co-initiator only resulted in small improvement of CQ absorption decay (Figure 6a-g), with τ values (Figure 7a) comparable to that of tertiary amines. Such observations are likely attributed to the competing light effect induced by NPG which may have affected the quantum yield of conversion of CQ molecules.

With an exception to NPG, resin model systems containing tertiary amines, particularly EDMAB-based formulations corresponded to the lowest τ values (1.0 mol %; Figure 7a), probably due to the highly reactive nature of aromatic amine-derived free radicals, as evidenced by a rapid CQ absorption coefficient decay at each concentration when compared with DMAEMA, BZD, and PA (Figure 6a-g). However (unlike cyclic acetals), a decrease in τ with successive EDMAB concentration was not strictly observed, and remained constant with little or no decrease, irrespective of EDMAB concentration (1.0 mol % CQ; Figure 7a). On the contrary, τ varied significantly for EDMAB-based formulations involving low (0.5 mol %) and high CQ (1.5 mol %) concentrations (Supplementary 1A), which may be due to insufficient and surplus amounts of CQ:amine mixture in the resin model system, respectively.

Except for 0.5 molar equivalent concentration, DMAEMA generally exhibited a more gradual decrease in τ with reciprocal increase in the ϕ of CQ conversion, at successive concentrations (Figure 7). This was also observed for low (0.5 mol %) and high (1.5 mol %) CQ concentrations, irrespective of the decreased DC and reaction rates mentioned previously (Section 4.1).

The steady increase in QY of conversion of CQ and mutual decrease in τ values (Figure 7), involving both cyclic acetals (BZD and PA), might be attributed to the photon absorption during irradiation. It is proposed that the systematic screening to identify optimal co-initiator concentration in terms of maximum post-irradiation DC (%) along with 'effective' photon absorption for free-radical polymerisation may only be applicable involving low co-initiator concentrations. Equally, the use of inadequate CQ concentration may also lead to reaction inefficiencies. At low CQ concentration (0.50 mol %), insufficient CQ molecules may have been the limiting factor in generating enough free radical

species to initiate new growth centres in the resin mixture. Likewise, excess amount (1.5 mol %) may have led to CQ saturation and resulted in insufficient irradiation for complete conversion of CQ (Supplementary 1A), and thus further augmenting system constraints.

Differences in ϕ values of CQ between amine and cyclic acetal-based formulations might be attributed to the former, not only acting as a proton source in the abstraction process, but also scavenging peroxy intermediates that are formed when oxygen reacts with radical sites [47, 52]. As such, higher polymerisation rates, greater post-irradiation DC and consequently higher ϕ was achieved. On the other hand, cyclic acetal radicals might rearrange rapidly by b-scission to corresponding ester-end radicals, some of which are known to convert to inactive radicals via hydrogen migration [53], and may therefore also explain the relatively inferior polymerisation characteristics discussed above (Section 4.1)

In comparison with cyclic acetals and DMAEMA, variations and relatively higher ϕ of conversion of CQ/NPG-based formulations can be assigned to the competitive absorption effects of NPG over CQ, as evidenced by its absorption spectrum overlapping with that of CQ around 420-500 nm (Figure 3a). This may have influenced the total number of photons absorbed during irradiation and therefore affected the ϕ of conversion of CQ calculations. This seems plausible as, unlike cyclic acetals, variations and the inverse relationship of t to ϕ was not followed (Figure 7).

4.3 Cell Assay

The current study utilised MTT assay to evaluate the response of a biological system (HDPCs) following indirect exposure (released eluates) to the model photopolymer system containing the tested co-initiators. Equally, the use of UV light for curing model resin without photoinitiator, was to provide a baseline to assess cytotocxity caused by resin alone. Significant reduction in metabolic activity of cells treated with neat resin model media eulates is in agreement with previous cytotoxic studies documented on dental monomers involving a variety of cell types [5, 53-55]. Consequently, their contributory effects were taken into account when assessing the proposed co-initiators in the current investigation. It is has been documented that, beside cell cycle, dental monomers also effect cell proliferation and survival. TEGDMA has shown to act as a vasorelaxant, causing apoptosis and necrosis [5, 8, 53-57]. Likewise, relatively low metabolic activity from the CQ-only treated group (without co-initiator) (Figure 8) might be related to significantly low DC (%) of the resin model system, since CQ has shown to be relatively non-cytotoxic at low concentrations (< 1 mM) [6] with EC_{50} of 8 mM [56] involving HDPCs. The concentration of CQ in present work was 0.08 mM, well below both thresholds [56].

Equally, glycine derivatives such as NPG, are amino acids and have been reported to be biologically less toxic [42, 44, 45]. Cytocompatility effects of NPG presented herin reflected such reports accordingly. Similarly, biological effects of DMAEMA concur with previous cytotoxicity studies conducted on human gingival fibroblast (HGF) cells, where DMAEMA inhibited cell growth at elevated concentrations (> 1 mM) [58].

Finally, both cyclic acetals exhibited relatively low cytotoxicity, when compared with amine groups. The current results are in agreement with published data [21], wherein similar cytotoxic effects were observed for BZD and PA involving indirect biological assessment.

5 Conclusions

Both cyclic acetals have shown to be capable of facilitating photo-induced free radical polymerisation reactions. Being natural components with relatively less cytotoxicity compared with their amine counterparts, their use as alternative co-initiators could potentially realise biological improvement with reduced cytotoxicity of photocurable resin-based dental and other biomaterials. Based on polymer conversion (DC), the optimal molar ratio of BZD and PA to CQ appeared to be 4:1. However, further formulation studies on CQ and alternative co-initiators are necessary in order to establish concentrations that would result in polymerisation rates and ϕ of conversion of CQ analogous to conventionally used amines.

The role of NPG as a co-initiator resulted in DC and reaction rates that are comparable with that of EDMAB. However, its competitive absorption would limit its use to low concentrations (below 2 molar equivalent (%) in the resin mixture). Based on current findings, the optimal concentration of EDMAB and DMAEMA, involving unfilled low viscosity model resin mixture, are 3.5-to-4 and 2 molar equivalent (%), respectively. Beyond these concentrations, negligible improvement in DC, reaction rates and ϕ of CQ conversion was observed.

6 Declaration Interests

The authors declare no competing interests.

7 Data Availability

All data supporting this study are present within the paper and supplementary file (Supplementary 1A).

8 Acknowledgments

AS Hamidi gratefully acknowledges financial support from EPSRC through a studentship from the Physical Sciences for Health Centre for Doctoral Training (EP/L016346/1).

9 References

[1] Kamoun EA, Winkel A, Eisenburger M, Menzel H. Carboxylated Camphorquinone as Visible-Light Photoinitiator for Biomedical Application: Synthesis, Characterization, and Application. Arabian Journal of Chemistry, 2016;9:745-754.

[2] Ferreira P, Coelho JFJ, Almeida JF, Gil MH. Photocrosslinkable Polymers for Biomedical Applications. In: Reza Afzal, editor. Biomedical Engineering - Frontiers and Challenges, Shanghai: InTech; 2011, p. 55-74.

[3] Leprince JG, Palin WM, Hadis MA, Devaux J, Leloup G. Progress in dimethacrylate-based dental composite technology and curing efficiency. Dental Materials, 2013;29(2):139-56.

[4] Santini A, Gallegos IT, Felix CM. Photoinitiators in dentistry: a review. Primary Dental Journal, 2013;2(4):30-33.

[5] Krifka S, Spagnuolo G, Schmalz G, Schweikl H. A review of adaptive mechanisms in cell responses towards oxidative stress caused by dental resin monomers. Biomaterials, 2013;34(19):4555-4563.

[6] Walters NJ, Xia W, Salih V, Ashley PF, Young AM. Poly(propylene glycol) and urethane dimethacrylates improve conversion of dental composites and reveal complexity of cytocompatibility testing. Dental Materials, 2016;32(2):264-277.

[7] Van Landuyt KL, Krifka S, Hiller K.-A, Bolay C, Waha C, Van Meerbeek B, et al. Evaluation of cell responses toward adhesives with different photoinitiating systems. Dental Materials, 2015; https://dx.doi.org/10.1016/j.dental.2015.04.016.

[8] Martins CA, Leyhausen G, Geurtsen W, Volk J. Intracellular glutathione: A main factor in TEGDMA-induced cytotoxicity? Dental Materials, 2012;28:442-448.

[9] Albuquerque PP, Moreira AD, Moraes RR, Cavalcante LM, Schneider LF. Color stability, conversion, water sorption and solubility of dental composites formulated with different photoinitiator systems. Journal of Dentistry, 2013;41(Suppl 3):67-72.

[10] Shin D-H, Rawls HR. Degree of conversion and color stability of the light curing resin with new photoinitiator systems. Dental Materials, 2009;25(8):1030-1038.

[11] Ural Ç, Duran I, Tatar N, Öztürk Ö, Kaya İ, Kavut I. The effect of amine-free initiator system and the polymerization type on color stability of resin cements. Journal of Oral Science, 2016; https://dx.doi.org/ 10.2334/josnusd.15-0619.

[12] Hadis MA, Shortall AC, Palin WM. Competitive light absorbers in photoactive dental resin-based materials. Dental Materials, 2012;28(8):831-841.

[13] Shi S, Nie J. A natural component as coinitiator for unfilled dental resin composites. Journal of Biomedical Materials Research. Part B, Applied Biomaterials, 2007;82(1):44-50.

[14] Matos MA, Monte MJ, Sousa CC, Almeida AR, Morais VM. Thermodynamic study of sesamol, piperonyl alcohol, piperonylic acid and homopiperonylic acid: a combined experimental and theoretical investigation. Organic & Biomolecular Chemistry, 2004;2(6):908-914.

[15] Lima GdS, Ogliari FA, Souza e Silva MG, Munchow EA, Petzhold CL, Piva E. Benzodioxoles as alternative coinitiators for radical polymerization in a model-dental adhesive resin. Journal of Applied Polymer Science, 2013;127(5):4160-4167.

[16] Tagashira M, Ohtake Y. A New Antioxidative 1,3-Benzodioxole from Melissa officinalis. Planta Medica, 1998;64(06):555-558.

[17] Mazzio EA, Harris N, Soliman KF. Food constituents attenuate monoamine oxidase activity and peroxide levels in C6 astrocyte cells. Planta Medica, 1998;64(7):603-606.

[18] Hodgson E, Philpot RM. Interaction of methylenedioxyphenyl (1,3-benzodioxole) compounds with enzymes and their effects on mammals. Drug Metabolism Reviews, 1974;3(2):231-301.

[19] Yokota S, Kitahara M, Nagata K. Benzylidene lactam compound, KNK437, a novel inhibitor of acquisition of thermotolerance and heat shock protein induction in human colon carcinoma cells. Cancer Research, 2000;60(11):2942-2948.

[20] Tseng TH, Tsheng YM, Lee YJ. Cytotoxicity effects of di- and tri-hydroxybenzaldehydes as a chemopreventive potential agent on tumor cells. Toxicology, 2001;161(3):179-187.

[21] Shi S, Xiao P, Wang K, Gong Y, Nie J. Influence of chemical structures of benzodioxole-based coinitiators on the properties of the unfilled dental resin. Acta Biomaterialia, 2010; 6(8): 3067-3071.

[22] Steingruber E. Indigo and Indigo Colorants, in Ullmann's Encyclopedia of Industrial Chemistry. 2004;19:55-63. https://doi.org/10.1002/14356007.a14_149.pub2.

[23] Kabatc J, Kucybala Z, Pietrzak M, Scigalski F, Paczkowski J. Free radical polymerization initiated via photoinduced intermolecular electron transfer process: kinetic study 3. Polymer, 1999;40(3):735-745.

[24] Kucybala Z, Paczkowski J. 3-Benzoyl-7-diethylamino-5-methyl-1-phenyl-1H-quinoxalin-2-one: An effective dyeing photoinitiator for free radical polymerization. Journal of Photochemistry and Photobiology A: Chemistry, 1999;128. https://doi.org/10.1016/S1010-6030(99)00158-6.

[25] Kucybaa Z, Pietrzak M, Paczkowski J, Linden L-A, Rabek JF. Kinetic studies of a new photoinitiator hybrid system based on camphorquinone-N-phenylglicyne derivatives for laser polymerization of dental restorative and stereolithographic (3D) formulations. Polymer, 1996;37(20):4585-4591.

[26] Wang Y, Spencer P, Yao X, Ye Q. Effect of coinitiator and water on the photoreactivity and photopolymerization of HEMA/camphoquinone-based reactant mixtures. Journal of Biomedical Materials Research. Part A, 2006;78(4):721-728.

[27] OceanOptics. USB4000-UV-VIS, https://oceanoptics.com/product/usb4000-uv-vis/; 2021 [Accessed 15th November 2021].

[28] Shortall AC, Hadis MA, Palin WM. On the inaccuracies of dental radiometers. PLoS One. 2021;16(1). https://doi.org/10.1371/journal.pone.0245830.

[29] Chen Y-C, Ferracane JL, Prahl SA. Quantum yield of conversion of the photoinitiator camphorquinone. Dental Materials, 2007;23(6):655-664.

[30] Cortes O, Garcia C, Perez L, Boj J, Alcaina A. Pulp cell cultures obtained with two different methods for in vitro cytotoxicity tests. European Archives of Paediatric Dentistry, 2006;7(2):96-99.

[31] Sittampalam GS. Assay guidance manual. Bathesda: Eli Lilly & Company and the National Center for Advancing Translational Sciences; 2016, p. 263-267.

[32] Hadis MA, Cooper PR, Milward MR, Gorecki PC, Tarte E, Churm J, et al. Development and application of LED arrays for use in phototherapy research. Journal of Biophotonics, 2017;10(11):1514-1525.

[33] SHIMADZU. The Relationship Between UV-VIS Absorption and Structure of Organic Compounds, https://www.shimadzu.com/an/uv/support/uv/ap/apl.html; 2019 [Accessed 10th October 2019].

[34] Polymer Database. Photodegradation of Polymers, https://polymerdatabase.com/polymer%20chemistry/Photo%20Oxidation.html; 2015 [Accessed 3rd July 2019].

[35] Speight JG. Chapter Seven - Transformation of Inorganic Chemicals in the Environment. In: Speight JG editor. Environmental Inorganic Chemistry for Engineers: Butterworth-Heinemann; 2017, p. 333-382.

[36] International Standard ISO 10993-12:2012.Biological evaluation of medical devices - Part 12: sample preparation and reference materials. Brussels: International Standards Organization; 2012.

[37] International Standardard ISO 10993-5:2009(E). Biological evaluation of medical devices - Part 5: tests for in vitro cytotoxicity. Brussels: International Standards Organization; 2009.

[38] Cook WD. Photopolymerization Kinetics of Dimethacrylates Using the Camphorquinone Amine Initiator System. Polymer, 1992;33(3):600-609.

[39] Kwon TY, Bagheri R, Kim YK, Kim KH,Burrow MF. Cure mechanisms in materials for use in esthetic dentistry. Journal of Investigative and Clinical Dentistry, 2012;3(1):3-16.

[40] Andrade KMGd, Palialol AR, Lancellotti AC, Aguiar FHB, Watts DC, Gonçalves LS, et al. Effect of diphenyliodonium hexafluorphosphate on resin cements containing different concentrations of ethyl 4-(dimethylamino)benzoate and 2-(dimethylamino)ethyl methacrylate as co-initiators. Dental Materials, 2016;32(6):749-755.

[41] Price RBT, Felix CA. Effect of delivering light in specific narrow bandwidths from 394 to 515nm on the micro-hardness of resin composites. Dental Materials, 2009;25(7):899-908.

[42] Al Mousawi A, Garra P, Schmitt M, Toufaily J, Hamieh T, Graff B, et al. 3-Hydroxyflavone and N-Phenylglycine in High Performance Photoinitiating Systems for 3D Printing and Photocomposites Synthesis. Macromolecules, 2018;51(12):4633-4641.

[43] Shi S, Gao H, Wu G, Nie J. Cyclic acetal as coinitiator for bimolecular photoinitiating systems. Polymer, 2007; 48(10):2860-2865.

[44] Ullrich G, Burtscher P, Salz U, Moszner N, Liska R. Phenylglycine derivatives as coinitiators for the radical photopolymerization of acidic aqueous formulations. Journal of Polymer Science Part A - Polymer Chemistry, 2006; 44:115-125.

[45] Zhang J, Lalevee J, Mou X, Morlet-Savary F, Graff B, Xiao P. N-Phenylglycine as a Versatile Photoinitiator under Near-UV LED. Macromolecules, 2018;51(10):3767-3773.

[46] Allonas X, Fouassier J-P, Angiolini L, Caretti D. Excited-State Properties of Camphorquinone Based Monomeric and Polymeric Photoinitiators. Helvetica Chimica Acta, 2001;84(9):2577-2588.

[47] Jakubiak J, Allonas X, Fouassier J-P, Sionkowska A, Andrzejewska E, Linden LA, et al. Camphorquinone–amines photoinitating systems for the initiation of free radical polymerization. Polymer, 2003;44:5219-5226.

[48] Mateo JL, Bosch P, Lozano AE. Reactivity of Radicals Derived from Dimethylanilines in Acrylic Photopolymerization. Macromolecules, 1994;27(26):7794-7799.

[49] Bowen RL, Argentar H. Tertiary Aromatic Amine Accelerators with Molecular Weights Above 400. Journal of Dental Research, 1972;51(2):473-482.

[50] Furuse AY, Mondelli J, Watts DC. Network structures of Bis-GMA/TEGDMA resins differ in DC, shrinkage-strain, hardness and optical properties as a function of reducing agent. Dental Materials, 2011;27(5):497-506.

[51] Neumann MG, Miranda WG, Schmitt CC, Rueggeberg FA, Correa IC. Molar extinction coefficients and the photon absorption efficiency of dental photoinitiators and light curing units. Journal of Dentistry, 2005;33(6):525-532.

[52] Fouassier JP and Lalevee J. Two-Component Photoinitiating Systems. In: Photoinitiators for Polymer Synthesis, Somerset DE:Wiley-VCH; 2012. https://doi.org/10.1002/9783527648245.ch9.

[53] Masuki K, Nomura Y, Bhawal UK, Sawajiri M, Hirata I, Nahara Y, et al. Apoptotic and Necrotic Influence of Dental Resin Polymerization Initiators in Human Gingival Fibroblast Cultures. Dental Materials Journal, 2007;26(6):861-869.

[54] Basak F, Vural IM, Kaya E, Ulku C, Guven G, Cehreli SB, et al., Vasorelaxant effect of a self-etch adhesive system through calcium antagonistic action. Journal of Endodontics, 2008;34(10):1202-6.

[55] Maddux WF, Abebe W, Schuster GS, Mozaffari MS. Effects of dental resin components on vascular reactivity. Journal of Biomedical Material Research, 2002;61(4):572-80.

[56] Van Landuyt KL, Krifka S, Hiller K.-A, Bolay C, Waha C, Van Meerbeek B, et al. Evaluation of cell responses toward adhesives with different photoinitiating systems. Dental Materials, 2015; Dental-2556. https://dx.doi.org/10.1016/j.dental.2015.04.016.

[57] Schweikl H, Hartmann A, Hiller K.-A, Spagnuolo G, Bolay C, Brockhoff G, et al. Inhibition of TEGDMA and HEMA-induced genotoxicity and cell cycle arrest by N-acetylcysteine. Dental Materials, 2007;23:688-695.

[58] Kumagai Y, Lin LY, Schmitz DA, Cho AK. Hydroxyl radical mediated demethylenation of (methylenedioxy)phenyl compounds. Chemical Research in Toxicology, 1991;4(3):330-334.